NIH Public Access
Author Manuscript
Immunity. Author manuscript; available in PMC 2013 August 24.

Published in final edited form as:
Immunity. 2012 August 24; 37(2): 249–263. doi:10.1016/j.immuni.2012.05.023.

Galectin-1 Deactivates Classically-Activated Microglia and Protects from Inflammation-Induced Neurodegeneration

Sarah C. Starossom[1,7], **Ivan D. Mascanfroni**[2,7], **Jaime Imitola**[1], **Li Cao**[1,3], **Khadir Raddassi**[1], **Silvia F. Hernandez**[2], **Ribal Bassil**[1], **Diego O. Croci**[2], **Juan P. Cerliani**[2], **Delphine Delacour**[4], **Yue Wang**[1], **Wassim Elyaman**[1], **Samia J. Khoury**[1,5,7,*], and **Gabriel A. Rabinovich**[2,6,7,*]

[1]Center for Neurologic Diseases, Brigham and Women's Hospital, Harvard Medical School, 02115 Boston, MA, USA

[2]Laboratorio de Inmunopatología, Instituto de Biología y Medicina Experimental (IBYME), Consejo Nacional de Investigaciones Científicas y Técnicas (CONICET), 1428 Buenos Aires, Argentina

[3]Department of Neurobiology, Institute of Neurosciences, Second Military Medical University, 200433 Shanghai, China

[4]Department of Developmental Biology, Institut Jacques Monod, CNRS 7592, Paris-Diderot University, Paris, France

[5]Abu Haidar Neuroscience Institute, American University of Beirut, Beirut, Lebanon

[6]Laboratorio de Glicómica Funcional, Departamento de Química Biológica, Facultad de Ciencias Exactas y Naturales, Universidad de Buenos Aires, 1428 Buenos Aires, Argentina

SUMMARY

Inflammation-mediated neurodegeneration occurs in the acute and the chronic phases of multiple sclerosis (MS) and its animal model experimental autoimmune encephalomyelitis (EAE). Classically-activated (M1) microglia are key players mediating this process. Here we identified Galectin-1 (Gal1), an endogenous glycan-binding protein, as a pivotal regulator of M1 microglia activation, targeting the activation of p38MAPK-, CREB-, and NF-κB-dependent signaling pathways and hierarchically supressing downstream pro-inflammatory mediators such as iNOS, TNF and CCL2. Gal1 bound to core 2 O-glycans on CD45, favoring retention of this glycoprotein on the microglial cell surface and augmenting its phosphatase activity and inhibitory function. Gal1 was highly expressed in the acute phase of EAE and its targeted deletion resulted in pronounced inflammation-induced neurodegeneration. Adoptive transfer of Gal1-secreting astrocytes or administration of recombinant Gal1 suppressed EAE through mechanisms involving microglia de-activation. Thus, Gal1-glycan interactions are essential in tempering microglia activation, brain inflammation and neurodegeneration with critical therapeutic implications for MS.

© 2012 Elsevier Inc. All rights reserved.

*Correspondence: skhoury@rics.bwh.harvard.edu (S.J.K.) or gabyrabi@gmail.com (G.A.R.) .
[7]These authors equally contributed to this work as co-first authors

SUPPLEMENTAL INFORMATION Supplemental Information includes seven figures and Supplemental Experimental Procedures.

Publisher's Disclaimer: This is a PDF file of an unedited manuscript that has been accepted for publication. As a service to our customers we are providing this early version of the manuscript. The manuscript will undergo copyediting, typesetting, and review of the resulting proof before it is published in its final citable form. Please note that during the production process errors may be discovered which could affect the content, and all legal disclaimers that apply to the journal pertain.

[8]These authors equally contributed to this work as co-senior authors

NIH-PA Author Manuscript
NIH-PA Author Manuscript
NIH-PA Author Manuscript

NIH-PA Author Manuscript

NIH-PA Author Manuscript

NIH-PA Author Manuscript

INTRODUCTION

Multiple Sclerosis (MS) is a chronic inflammatory demyelinating and degenerative disease of the central nervous system (CNS). The clinical disease course usually starts with reversible episodes of neurologic disability (relapsing-remitting MS; RRMS), which later goes into a progressive stage with irreversible neurologic decline (secondary progressive MS; SPMS) (Trapp and Nave, 2008). Axonal loss occurs in both the acute and chronic phases of MS and its animal model experimental autoimmune encephalomyelitis (EAE) and the loss of compensatory CNS mechanisms contributes to the transition from RRMS to SPMS (Zamvil and Steinman, 2003).

Activated microglia and macrophages are thought to contribute to neurodegeneration as their number correlates with the extent of axonal damage in MS lesions (Bitsch et al., 2000; Rasmussen et al., 2007) and with neuronal dysfunction in EAE (Weiner, 2009). Microglia and macrophages can be activated by the cytokines IFN-γ, IL-17 or lipopolysaccharide (LPS) into a pro-inflammatory phenotype (M1), while IL-4 or IL-13 induce a state of alternative activation (M2), which is associated with neuroprotective functions that promote repair (Ponomarev et al., 2007; Butovsky et al., 2006; Kawanokuchi et al., 2008).

Recent efforts toward decoding the information encoded by the 'glycome' revealed essential roles of glycan-binding proteins or lectins in the regulation of immune tolerance and inflammation (Rabinovich and Croci, 2012). Galectins, a family of endogenous lectins, function in the extracellular milieu by interacting with a myriad of glycosylated receptors on the surface of immune cells (Rabinovich and Croci, 2012). However, these lectins may also play roles inside the cells including modulation of intracellular signaling pathways. Although originally defined by their ability to recognize the disaccharide N-acetyllactosamine [Galβ(1–4)-GlcNAc; LacNAc], recent evidence indicates substantial differences in the glycan-binding preferences of individual members of the galectin family (Rabinovich and Croci, 2012). Galectin-1 (Gal1; encoded by *Lgals1* gene), has been implicated in the regulation of innate and adaptive immunity. In the periphery, Gal1 promotes selective apoptosis of Th1 and Th17 cells (Toscano et al., 2007), induces IL-10 secretion (van der Leij et al., 2007; Stowell et al., 2008; Cedeno-Laurent et al., 2012), inhibits T-cell trafficking (Norling et al., 2008) and decreases antigen-presenting capacity and nitric oxide (NO) production by macrophages (Barrionuevo et al., 2007; Correa et al., 2003). Furthermore, exposure to Gal1 promotes the differentiation of IL-27-producing tolerogenic dendritic cells (DCs) (Ilarregui et al., 2009) and favors the expansion of inducible T regulatory (iTreg) cells (Toscano et al., 2006); however the function of this lectin on endogenous CNS innate immunity is unknown.

Here we show that endogenous and exogenous Gal1 plays a pivotal role in deactivating classically-activated microglia and promoting a phenotype of alternative activation through modulation of p38-MAPK, CREB and NF-κB signaling pathways. This effect involved binding of Gal1 to core 2 O-glycans on CD45, which promoted retention of this glycoprotein on the microglial cell surface and augmented its phosphatase activity. *In vivo*, Gal1 prevented microglia activation and promoted neuroprotection. Our findings suggest a glycosylation-dependent mechanism for preventing inflammation-induced neurodegeneration through selective deactivation of microglial cells.

RESULTS

Dynamic Regulation of Endogenous Gal1 in CNS Cells

Gal1 expression in the spinal cord was analyzed at the mRNA level (Figure 1A) and at the protein level (Figures 1B and 1C) in the white matter of spinal cord tissue in naïve mice, and

NIH-PA Author Manuscript

NIH-PA Author Manuscript

NIH-PA Author Manuscript

in mice with MOG-induced EAE at preclinical stage (day 10 post-immunization), peak of disease (day 15-16 post-immunization) and chronic stage (day 30 to 40 post-immunization). In naïve mice, there was very little expression of Gal1 in the CNS, but during the preclinical phase Gal1 protein expression was increased (Figures 1B and 1C), while Gal1 mRNA expression was unchanged (Figure 1A). Gal1 expression was highest at the peak of disease and persisted at lower levels during the chronic phase of EAE (Figures 1A-C). Of note, Gal1 was highly expressed in $GFAP^+$ astrocytes bordering the lesion area (Figure 1D), in a subset of $CD4^+$ T cells (Figure 1E) and in a subset of $CD11b^+$ cells (Figure 1F) during preclinical and acute EAE. During the chronic phase of EAE only astrocytes maintained considerable expression of this lectin (Figure 1D).

These observations prompted us to investigate the potential stimuli that induce expression of this lectin. In astrocytes, we observed strong downregulation of Gal1 mRNA following stimulation with LPS or IL-17A, a slight increase after IFN-γ treatment and strong upregulation after exposure to anti-inflammatory stimuli such as IL-4, TGF-β_1 and Gal1 itself (Figure 1G). However, only stimulation of astrocytes with IL-4 and TGF-β_1 led to a significant increase in secreted Gal1 (Figure 1G).

We then analyzed Gal1 mRNA expression and Gal1 secretion in *in vitro* differentiated Th1, Th2, Th17 and iTreg cells, and Gal1 mRNA expression in *ex vivo*-isolated natural T regulatory (nTreg) cells. Gal1 mRNA was downregulated in Th1 and Th2 cells, but not in Th17 and iTreg cells as compared to non-polarized activated T cells (Th0) (Figure S1A). Moreover, there was a trend toward a decrease in Gal1 secretion in all subsets when compared to non-polarized T cells (Figure S1B). $FoxP3^+$ GFP^+ nTreg cells that were isolated from the spleen of naïve mice showed higher Gal1 mRNA expression compared to $FoxP3^-$ GFP^- cells (Figure S1C). Similarly, $FoxP3^+$ $CD4^+$ T cells isolated from the CNS showed increased Gal1 expression compared to the $FoxP3^-$ population during preclinical and acute EAE (Figure S1D), although both populations had increased expression during acute EAE compared to preclinical EAE.

Similar to our observations in astrocytes, anti-inflammatory or Th2 cell-type stimuli led to substantial upregulation of Gal1 mRNA expression and secretion in microglia, whereas Gal1 mRNA was downregulated upon exposure to LPS or IFN-γ (Figures S1E and S1F). Exposure to IL-17A did not affect Gal1 mRNA expression or Gal1 secretion. Furthermore, Gal1 itself slightly increased Gal1 mRNA expression (Figure S1E), suggesting that Gal1 might act in an autocrine manner to control microglial responses.

Gal1 Controls M1 Microglia Activation through Modulation of p38MAPK, CREB and NF-κB Signaling Pathways

Activation with LPS or IFN-γ induces an M1 phenotype in microglial cells that is characterized by high MHC II, CD86 and inducible nitric oxide (iNOS) expression and production of pro-inflammatory cytokines and chemokines such as TNF and CCL2, whereas stimulation with IL-4 induces an M2 phenotype characterized by arginase expression (Ponomarev et al., 2007). We investigated the binding of Gal1 to M1 or M2 microglia. Gal1 bound to isolated primary microglia in a dose- and saccharide-dependent fashion (Figures 2A and S2). Gal1 binding was markedly increased when microglia were polarized toward an M1 phenotype (Figure 2A). In contrast, Gal1 binding to M2-polarized microglia was substantially decreased compared to unstimulated microglia (Figure 2A). To determine whether differential binding to M1- or M2-activated microglia correlates with distinct ‘glycosylation signatures’, we compared the glycophenotype of these cells using a panel of plant lectins that selectively recognize specific oligosaccharide sequences (Toscano et al., 2007). Whereas *Sambucus nigra agglutinin* (SNA) recognizes α2-6-linked sialic acid which interferes with Gal1 binding, *Maackia amurensis* agglutinin (MAL II) binds to α2-3 sialic

NIH-PA Author Manuscript

NIH-PA Author Manuscript

NIH-PA Author Manuscript

acid linkages, L-phytohemagglutinin (L-PHA) recognizes β1-6 branching on complex *N*-glycans, peanut agglutinin (PNA) recognizes asialo-galactose β1-3-N-acetylgalactosamine (core-1) *O*-glycans and *Helix pomatia* (HPA) binds specifically to terminal α-N-acetylgalactosamine residues (Hirabayashi et al., 2002). Notably, we found augmented unsialylated core 1 *O*-glycans in M1 (LPS or IFN-γ)-polarized compared to M2 (IL-4)-polarized microglia, as shown by abundant reactivity of these cells to PNA. Augmented PNA reactivity indicates increased availability of glycan structures required for elongation of core 2 *O*-glycans through the action of the core 2 β1,6-N-acetylglucosaminyltransferase 1 (C2GnT1), which favors LacNAc incorporation and galectin binding (Tsuboi et al., 2011). In addition, M1 microglia showed higher binding capacity to L-PHA, suggesting increased β1,6 branching of complex *N*-glycans (ligands for galectins) that are generated by the enzyme β1,6 N-acetylglucosaminyltransferase 5 (GnT5) (Partridge et al., 2004). This lectin-binding pattern was accompanied by higher HPA reactivity in M1 versus M2 microglia. Also, there was a trend toward higher binding of SNA to M2 microglia consistent with the well-recognized ability of α2-6-linked sialic acid to interfere with Gal1 binding. Finally, both M1- and M2-polarized microglia had similar binding profiles for MAL II, although IFN-γ-stimulated cells had lower MAL II binding. As α2,3-linked sialic acid may allow binding of Gal1 with different affinities than asialo-LacNAc structures (Hirabayashi et al., 2002), these results suggest that subtle differences may exist in the glycoprofile of different subpopulations of classically-activated (LPS or IFN-γ) microglia (Figure 2B). Collectively, these findings suggest that M1, but not M2 microglia, express the prefered set of glycans required for Gal1 binding and function.

To determine whether Gal1 binding to microglia results in phenotypic or functional changes, we first analyzed the cell surface phenotype of these cells. In IFN-γ-polarized M1 microglia, surface expression of MHC II and CD86 was substantially decreased following exposure to recombinant Gal1 (Figure 2C). Furthermore, expression of iNOS mRNA and production of TNF and CCL2 were significantly decreased by Gal1 in M1 microglia (Figures 2D-F and S3A-C). In contrast, M2-polarized microglia experienced a relative increase in arginase and iNOS mRNA compared to unstimuated microglia; yet exposure to Gal1 (at its highest dose) enhanced arginase mRNA expression but decreased iNOS mRNA expression (Figures 2G and 2H). This effect was also observed in LPS-stimulated Gal1-treated microglia (Figure S3D). Although Gal1 selectively deletes Th1 and Th17 cells (Toscano et al., 2007), we could find no effect of this lectin on the viability of microglial cells at concentrations ranging from 1 to 10 μg/ml (data not shown).

The production of NO and TNF is controlled by pro-inflammatory signaling pathways involving nuclear factor-κB (NF-κB) (Zhang et al., 2010), extracellular signal-regulated kinase (ERK) (Cui et al., 2010), p38 mitogen-activated protein kinase (p38MAPK) (Xing et al., 2008) and cAMP response element binding (CREB) (Mirzoeva et al., 1999). We investigated the effect of Gal1 on the phosphorylation of these signaling molecules in primary microglia cells from wild type (WT) and Gal1-deficient (*Lgals1*$^{-/-}$) mice. LPS induced phosphorylation of the inhibitor of κB-α (IκB-α), a negative regulator of the NF-κB pathway, after 5 min, and of p38-MAPK, ERK and CREB after 15 min of incubation (Figure 2I-M). However, activation of microglia with LPS in the presence of Gal1 induced a significant decrease in the phosphorylation of p38, CREB and IκB-α, but only slight inhibition in the phosphorylation of ERK (Figure 2I-M). Thus, Gal1 acts by limiting microglia activation mainly through modulation of p38-, CREB- and NF-κB-dependent pathways. Notably, there were no significant differences in the phosphorylation pattern of WT and *Lgals1*$^{-/-}$ microglia exposed to Gal1 (Figure 2I-M), suggesting that cell intrinsic Gal1 does not play a substantial role in the modulatory effects of exogenous Gal1.

NIH-PA Author Manuscript

NIH-PA Author Manuscript

NIH-PA Author Manuscript

Gal1 Promotes Retention of CD45 on the Surface of Microglial Cells and Augments its Phosphatase Activity

CD45 is a heavily glycosylated protein tyrosine phosphatase that negatively regulates M1 microglia activation, leading to the promotion of an M2 phenotype (Salemi et al., 2011). Because Gal1 binds to CD45 on T cells (Earl et al., 2010), we hypothesized that Gal1-glycan interactions may promote microglia de-activation by specifically retaining CD45 on the cell surface, thereby augmenting its phosphatase activity and prolonging transmission of inhibitory signals. Co-immunoprecipitation experiments with lysates of BV-2 microglia cells treated with Gal1 revealed specific interactions between Gal1 and CD45 (Figure 3A). Supporting these findings, exogenously-added Gal1 co-localized with CD45 on M1 microglial cells (Figure 3B). Notably, flow cytometric analysis of non-permeabilized cells demonstrated time-dependent retention of CD45 on the surface of LPS-stimulated M1 microglia exposed to Gal1 compared to cells treated with vehicle control (Figure 3C). This resulted in de-activation of M1 microglia, as shown by the time-dependent inhibition of CD80 expression (Figure 3D). Furthermore, Gal1-treated M1 microglia had considerably diminished co-localization of CD45 with EEA1 (an early endosomal marker) by confocal microscopy compared to LPS-stimulated microglia treated with vehicle control (Figure 3E), consistent with decreased internalization of CD45. Functionally, binding of Gal1 to CD45 resulted in a time-dependent increase in phosphatase activity (Figure 3F). This effect was eliminated in the presence of a CD45-specific phosphatase inhibitor (Figure 3F), indicating that increased phosphatase activity was completely attributed to CD45. To dissect the contribution of N- and O-glycans to this effect, we transfected BV-2 microglia cells with short interfering RNA (siRNA) for C2GnT1 and GnT5, two critical glycosyltransferases required for biosynthesis of Gal1 ligands (Figure S4). Inhibition of core 2 O-glycan elongation through siRNA-mediated silencing of C2GnT1 almost completely eliminated CD45-Gal1 interactions (Figure 3G) and Gal1-induced CD45 phosphatase activity (Figure 3H), whereas interruption of complex-type N-glycan branching through siRNA-mediated GnT5 silencing had no effect (Figures 3G and 3H). Thus, O-glycan-dependent binding of Gal1 to CD45 promotes retention of this glycoprotein on the surface of microglia cells and augments its phosphatase activity.

Lack of Endogenous Gal1 Enhances Classical Microglia Activation and Promotes Axonal Damage *in vivo*

Activated microglia may contribute to CNS pathology or repair depending on the prevalent microenvironment and their mode of activation. Whereas classically-activated M1 microglia is involved in inflammation-mediated neurotoxicity, alternatively-activated M2 microglia has neuroprotective functions (Kigerl et al., 2009). To investigate the role of Gal1 in microglia activation *in vivo*, we induced EAE in *Lgals1*$^{-/-}$ and WT mice. Iba^{+} MHC II^{+} microglia were considerably more abundant in *Lgals1*$^{-/-}$ mice when compared to WT EAE mice (Figure 4A), while healthy control mice had no Iba1^{+} MHC II^{+} cells in the CNS (data not shown). Furthermore, *Lgals1*$^{-/-}$ mice had decreased immunoreactivity against the neuronal and axonal marker β-III-tubulin (Tuj1) (Figure 4B), GAP43 (a marker for axonal growth cones) (Figure 4C) and myelin basic protein (MBP; a marker of myelination) (Figure 4D). In addition, *Lgals1*$^{-/-}$ mice showed increased GFAP^{+} astrocytes during ongoing EAE (Figure 4E). Thus, targeted deletion of endogenous Gal1 significantly increases axonal loss and decreases axonal outgrowth during autoimmune neuroinflammation.

Gal1 Controls Microglia-Mediated Neurotoxicity

To gain insight into the functional consequences of Gal1-induced microglia de-activation, we used an *in vitro* model of microglia-mediated neurotoxicity (Lehnardt et al., 2003). Neurons were co-cultured with resting microglia, or microglia pre-activated by LPS in the absence or presence of recombinant Gal1 or Gal1 alone. Since neurotoxicity is closely

NIH-PA Author Manuscript

NIH-PA Author Manuscript

NIH-PA Author Manuscript

associated with a collapse of cytoskeleton proteins (Takeuchi et al., 2005), we measured the intensity of immunoreactivity against microtubule-associated protein 2 (Map2), the density of $Map2^+$ cells and the percentage of beaded axons. Co-culture with LPS-activated microglia resulted in decreased neuronal density with lower Map2 immunoreactivity and higher percentage of beaded axons (Figure 5A-D). Interestingly, co-culture with microglia pre-activated with LPS and Gal1 showed significantly better preservation of neurons (Figure 5A-D). Moreover, Gal1-treated resting microglia behaved like resting microglia (Figure 5A-D). Similar results were observed with the microglia cell line BV-2 (Figure S5A-D). Furthermore, direct addition of Gal1 to neuronal cultures had no major effect as the density of surviving neurons, collapse of the cytoskeleton protein Map2 and axonal beading were not significantly altered (Figure S5E-H). Thus, Gal1 provides neuroprotection though deactivation of M1 microglia.

Astrocytes Control Microglia Activation via Gal1

As astrocytes express substantial amounts of Gal1 during both the acute and chronic phases of EAE (Figure 1D), we investigated whether Gal1 contributes to astrocyte-mediated control of microglia activation. We stimulated *Lgals1*$^{-/-}$ or WT neonatal astrocytes with PBS or TGF-β_1. Exposure to TGF-β_1 led to higher expression and secretion of Gal1 by astrocytes compared to astrocytes cultured with vehicle control (Figure 1G). The resulting astrocyte conditioned medium was transferred to cultures of IFN-γ-activated neonatal M1 microglia. There were no significant differences in MHC II expression in microglia incubated with conditioned media from WT or *Lgals1*$^{-/-}$ astrocytes exposed to vehicle control. However, M1 microglia that had been exposed to conditioned media from TGF-β_1–treated WT astrocytes showed decreased activation, whereas transfer of conditioned medium from TGF-β_1–treated *Lgals1*$^{-/-}$ astrocytes resulted in increased microglia activation (Figure 6A).

To test this hypothesis *in vivo*, we injected neonatal astrocytes (5×10^5/mouse) from *Lgals1*$^{-/-}$ or WT mice into the right lateral ventricle of *Lgals1*$^{-/-}$ mice with EAE when they reached a clinical score of 1 (Figures 6B and S6). Adoptive transfer of Gal1-sufficient astrocytes to EAE recipient *Lgals1*$^{-/-}$ mice successfully limited the severity of the disease, while injection of *Lgals1*$^{-/-}$ astrocytes failed to rescue disease phenotype (Figure 6C). However, WT astrocytes could not exert this suppressive effect when adoptively transferred to *Lgals1*$^{-/-}$ recipient mice which have been previously injected (days 7 and 9) with clodronate-containing lyposomes to deplete the microglia and macrophage compartments (Figure 6C). These data identify a CNS regulatory circuit by which astrocytes contribute to the resolution of autoimmune neuroinflammation via Gal1-dependent control of microglia activation.

Gal1 Therapy Decreases Microglia Activation and Prevents Neurodegeneration and Demyelination

To investigate whether Gal1 therapy influences EAE neuropathology, we initiated treatment around the onset of clinical disease (day 9 to 13 post-immunization) after inflammatory cells have already entered the CNS. Administration of Gal1 significantly attenuated EAE severity (Figures 7A and 7B) and decreased microglia activation in the spinal cord (Figure 7C). Accordingly, axonal damage, neuronal degeneration and demyelination were substantially reduced in Gal1-treated mice as reflected by increased staining of β-III-tubulin (Tuj1), GAP43 and MBP (Figures 7D-F). Furthermore, Gal1 treatment also reduced GFAP immunoreactivity (Figure 7G). Of note, administration of recombinant Gal1 to WT mice or transfer of Gal1-expressing astrocytes in *Lgals1*$^{-/-}$ EAE recipient mice also limited the viability of CNS mononuclear cells even in the absence of microglia (Figure S7), suggesting multiple cellular targets of Gal1 effects.

NIH-PA Author Manuscript

NIH-PA Author Manuscript

NIH-PA Author Manuscript

To definitely implicate microglia in the beneficial effects of Gal1 on EAE, we stimulated neonatal microglia with LPS, Gal1 or LPS plus Gal1 for 24 h and injected them (5×10^5 / mouse) into the right lateral ventricle *of Lgals1*$^{-/-}$ mice on day 9 post-immunization (Figure 7H). Transfer of LPS-treated microglia resulted in worsening of the clinical score compared to untreated microglia (Figure 7I). Remarkably, transfer of microglia treated with both LPS and Gal1 significantly ameliorated clinical disease compared to LPS-treated microglia. Furthermore, transfer of Gal1-treated resting microglia resulted in an even lower clinical disease course compared to untreated resting microglia (Figure 7I), suggesting that Gal1 treatment may prevent the *in vivo* activation of microglia after intracranial transfer.

DISCUSSION

In this study we identified a CNS regulatory circuit, mediated by Gal1-glycan interactions, that contributes to neuroprotection by deactivating classically-activated microglia and inducing an alternative M2 microglia phenotype. Endogenous Gal1 was up-regulated in preclinical EAE, peaked during acute EAE and remained elevated though to a lesser extent during the chronic phase of the disease. While during preclinical and acute EAE, Gal1 was expressed by astrocytes and a subpopulation of $CD4^+$ T cells and $CD11b^+$ cells, during chronic EAE its expression was mainly restricted to astrocytes. Furthermore, anti-inflammatory stimuli, including Gal1 itself, increased Gal1 synthesis by astrocytes, an effect which was critical in limiting microglia activation. Interestingly, we observed increased GFAP immunoreactivity in the inflamed CNS of *Lgals1*$^{-/-}$ mice and decreased GFAP reactivity following Gal1 treatment. In this regard, previous studies indicated that Gal1 promotes astrocyte maturation and inhibits astrocyte proliferation *in vitro* (Sazaki et al., 2004). Thus, it is likely that in addition to microglial cells, astrocytes may also respond to Gal1 and contribute to disease modulation by promoting a neuroprotective microenvironment. Moreover, our data show that CNS infiltrating $FoxP3^+$ Treg cells express more Gal1 than $FoxP3^-$ effector T cells during preclinical disease in accordance with the suggested role of Gal1 as a mediator of the immunosuppressive function of Treg cells (Garin et al., 2007).

Classically-activated microglia are associated with neurodegeneration, whereas alternatively-activated microglia have been shown to be anti-inflammatory and neuroprotective (Kigerl et al., 2009). We found that Gal1 displayed a significantly higher affinity to M1-type microglia, which respond to this lectin by down-regulating activation markers, pro-inflammatory cytokines and iNOS expression and by up-regulating markers that are otherwise only seen in M2-type microglia such as arginase. In the absence of endogenous Gal1, classical microglia activation is favored, concurrent with an increase in demyelination and axonal loss and a reduction in endogenous synaptic repair.

Within CNS inflamed tissues, $Iba1^+$ cells may be represented either by microglia or by peripheral macrophages. Gal1 is known to suppress macrophage activation in the periphery (Barrionuevo et al., 2007); thus it is likely that both microglia and macrophages in the CNS will respond to Gal1 with a decrease in classical activation. In this regard, it has been demonstrated that type II monocytes are critical for the resolution of brain inflammation (Weber et al., 2007), suggesting that Gal1 may contribute to this immunoregulatory effect. Likewise, other members of the galectin family have also been associated with the control of CNS microglia. This is the case of Gal3 which is up-regulated in microglia in response to ischemic brain lesions and favors myelin phagocytosis (Walther et al., 2000; Rotshenker et al., 2008) and Gal9 that signals through Tim-3 on $CD11b^+$ CNS cells to stimulate innate immunity (Anderson et al., 2007). Furthermore, Gal3 and Gal4 are highly expressed in oligodendrocytes, favor remyelination and contribute to amplifying CNS inflammatory responses (Pasquini et al., 2011; Wei et al., 2007; Stancic et al., 2012; Jiang et al., 2009;

NIH-PA Author Manuscript

NIH-PA Author Manuscript

NIH-PA Author Manuscript

Jeon et al., 2010). Strikingly, cell surface binding of Gal1 as well as the glycoprofile of classically-activated microglia recapitulate the pattern observed on Th1, Th17 cells and mature DCs, while the repertoire of cell surface glycans observed on alternatively-activated microglia is much more similar to that displayed by Th2 cells and immature DCs (Toscano et al., 2007; Bax et al., 2007).

Emerging evidence indicates that multivalent lectin-glycan interactions function by trapping glycoprotein receptors at the cell surface and preventing their endocytosis. This effect enhances receptor responsiveness to extracellular inputs and prolongs intracellular signaling (Rabinovich and Croci, 2012). Illustrating this concept, interactions between Gal3 and GnT5-modified N-glycans on TGF-βR or CTLA-4 (Partridge et al., 2004; Lau et al., 2007) and binding of Gal9 to complex N-glycans on the glucose transporter GLUT-2 (Ohtsubo et al., 2005) act by prolonging cell surface half life of these receptors. Here we found that Gal1 bound to core 2 O-glycans decorating CD45 on microglial cells, leading to retention of this glycoprotein on the plasma membrane and augmenting its phosphatase activity. In line with these findings, recent studies demonstrated that CD45 negatively regulates M1 microglia activation leading to the promotion of an M2 phenotype (Salemi et al., 2011). However, CD45 phosphatase activity is also target of the immunoregulatory activity of Gal1 and the macrophage galactose lectin (MGL) within the T cell compartment (Earl et al., 2010, van Vliet et al., 2006). Interestingly, O-glycosylation may dampen immune responses not only by preventing receptor internalization, but also by blocking receptor-ligand interactions. Binding of Gal3 to core 2 O-glycans decorating tumor-associated major histocompatibility complex class I-related chain A (MICA) reduces the affinity of MICA for the NKG2D receptor and impairs NK cell activation (Tsuboi et al., 2011). Thus, lectin-glycan interactions can adjust thresholds of cellular activation and survival by modulating endocytosis, trafficking and signaling of canonical receptors.

Our results demonstrate that Gal1 indirectly decreased neuronal loss through mechanisms involving p38-MAPK-, CREB- and NF-κB-dependent signaling pathways which are activated upstream of the neurotoxic molecules TNF and NO in the microglia. Notably, in our experiments, we found no direct effect of Gal1 on cultured neurons, different from a previous report on neurons derived from engineered mouse embryonic stem cells (Plachta et al., 2007). The divergence with our findings may be related to the source and biochemical properties of Gal1 used, including prevalence of monomeric versus dimeric or oxidized versus reduced forms of the protein. The degeneration of peripheral neuronal processes in *Lgals1*$^{-/-}$ mice may be due to the loss of endogenous neuron-derived Gal1 or to differences between the peripheral nervous system and the CNS.

Several circuits, mediated by astrocytes and microglia, were reported to modulate CNS inflammation, including those involving Act1, a critical component of IL-17 signaling (Kang et al., 2010). We found that IL-17 did not considerably alter Gal1 expression in microglia or astrocytes. However, given the relevance of the IL-17-IL-17R axis in CNS pathology (Kang et al., 2010; Kawanokuchi et al., 2008), future studies are warranted to examine the cross-talk between Gal1 and IL-17 signaling in inflammation-induced neurodegeneration

In summary, we identified a CNS regulatory circuit by which astrocytes negatively regulate microglia activation and temper disease severity through Gal1-dependent mechanisms. Our data confirm a protective role of Gal1 in autoimmune inflammation (Offner et al., 1990; Toscano et al., 2007) and demonstrate that EAE amelioration and the underlying mechanisms of neuroprotection are mediated by inactivation of M1 microglia, suggesting that the establishment of Gal1-glycan interactions among different glial cells may provide an endogenous mechanism to limit neuropathology. Thus, targeting the Gal1-glycan axis may

NIH-PA Author Manuscript

NIH-PA Author Manuscript

NIH-PA Author Manuscript

represent a new therapeutic approach for diseases involving inflammation-associated neurodegenedration, such as MS as well as Alzheimer's and Parkinson's disease.

EXPERIMENTAL PROCEDURES

Mice and EAE Induction

Female C57BL/6 mice were purchased from the Jackson Laboratory (Bar Harbor, ME). *Lgals1*$^{-/-}$ mice (C57BL/6) were provided by F. Poirier (Institute Jacques Monod, Paris). The encephalitogenic MOG35-55 peptide (M-E-V-G-W-Y-R-S-P-F-S-R-V-V-H-L-Y-R-N-G-K) was synthesized by Biopolymer Lab (University of California, Los Angeles, CA) and purified to >99% by HPLC. *Lgals1*$^{-/-}$ and WT mice were immunized subcutaneously in two sites (left and right flanks) with 150 μg of MOG35-55 peptide that was emulsified in complete Freund's adjuvant (CFA; Sigma, St Louis, MO) containing 200 μg *Mycobacterium tuberculosis* (Difco, Detroit, MI). Mice received 200 ng pertussis toxin (PT, List Biological, Campbell, CA) in 0.2 ml PBS by intraperitoneal (i.p.) injections at the time of immunization and 48 h later. Control mice were immunized with CFA followed by PT. Mice are scored daily as follows: 0, no disease; 1, loss of tail tone; 1.5, poor righting ability; 2, hind limb weakness; 3, hind limb paralysis; 4, quadreparesis; 5, moribund. All animals were housed in pathogen-free facilities at the Institute of Biology and Experimental Medicine (Buenos Aires, Argentina) or at the New Research Building, Harvard Medical School (Boston, MA) according to NIH guidelines. All experiments were performed with the approval of the Harvard Medical Area Standing Committee on Animals and the Institutional Review Board of the Institute of Biology and Experimental Medicine.

Preparation of Recombinant Gal1

Purification of recombinant Gal1 was accomplished as outlined previously (Barrionuevo et al., 2007). Potential LPS contamination was carefully removed by Detoxi-Gel™ (Pierce) and tested using with a Gel Clot Limulus Test (< 0.5 IU/mg; Cape Code).

Isolation and Culture of Microglia and Astrocytes

Brains from neonatal C57BL/6 WT or *Lgals1*$^{-/-}$ mice (P0-P2) were stripped of their meninges and minced in Ca^{2+}-free HBSS. Neural tissue was digested using the Neural Tissue Dissociation Kit (P) (Miltenyi Biotec). The cell suspension was cultured in microglia culture medium (DMEM with 10% fetal bovine serum (FBS), penicillin (50 U/ml), streptomycin (50 μg/ml), sodium pyruvate (1 mM) and L-glutamine (2 mM) at 37°C and 5% CO_2. Fresh medium was added to the culture every 2 days for a total period of 10-14 days. Neonatal microglia cells were shaken off the mixed brain glia cell culture after 10 to 14 days (150 rpm, 37°C, 6 h). Microglia cells were washed and subjected to further analysis. Astrocytes for *in vitro* use were isolated as described (Wang et al., 2008). Astrocytes for *in vivo* transfer were isolated using ACSA-1 MicroBead Kit (Miltenyi Biotec). The anti-ACSA-1 (Astrocyte Cell Surface Antigen-1) antibody is specific for the astrocyte transmembrane glycoprotein GLAST (Storck et al., 1992). Purity of astrocyte preparations was checked using an anti-GFAP antibody (BD Biosciences). Astrocytes or microglia were stimulated with LPS (10 ng/ml), IFN-γ (10 ng/ml), IL-17 (10 ng/ml), IL-4 (10 ng/ml), IL-13 (10 ng/ml), TGF-β_1 (5 ng/ml) or Gal1 (5 μg/ml) for 48 h. Samples were stored at –80°C until subjected to further analysis. Most *in vitro* de-activation experiments, particularly those involving primary isolated microglia, were performed by pre-incubating cells with Gal1 for short periods (15 min to 2 h) before adding LPS, whereas experiments using BV-2 microglia cells (CD45 retention, endocytosis, phosphatase activity and phenotypic markers) were conducted either by pre-incubating, co-incubating or adding Gal1 for different time periods after LPS treatment, giving similar results.

NIH-PA Author Manuscript

NIH-PA Author Manuscript

NIH-PA Author Manuscript

Immunoblotting and Co-immunoprecipitation

Primary neonatal microglia from WT and *Lgals1*$^{-/-}$ mice were pre-incubated with or without recombinant Gal1 (25 μg/ml) for 15 min followed by stimulation with LPS (100 ng/ml). Cells were then washed, lysed and subjected to immunoblot analysis using antibodies against phosphorylated and unphosphorylated signaling molecules (all from Cell Signaling) as described (Ilarregui et al., 2009). For co-immunoprecipitation, 500 μg cell lysates were incubated with 2 μg anti-CD45 or isotype control antibodies (eBiosciences). The immunocomplexes were captured with Protein G PLUS-Agarose (Santa Cruz Biotechnol) and processed for immunoblotting.

Flow Cytometry and Glycophenotypic analysis

For assessment of Gal1 binding, recombinant Gal1 was pre-absorbed with biotinylated anti-Gal1 antibody (R&D) overnight at 4°C. Pre-stimulated microglia cells were incubated with increasing concentrations of pre-absorbed Gal1 in the absence or presence of lactose or sucrose for 1 h at 37°C. Cells were then incubated with allophycocyanin (APC)-conjugated streptavidin (BD Biosciences) for 15 min at 4°C. For glycophenotyping, microglia cells were stimulated with or without LPS, IFN-γ or IL-4 for 24 h and then stained with biotinylated SNA (20 μg/ml; Vector), PNA (20 μg/ml; Sigma), L-PHA (2 μg/ml; Vector), HPA (20 μg/ml; Sigma) or MAL II (5 μg/ml; Vector) followed by fluorescein isothiocyanate (FITC)-conjugated strepatavidin. Nonspecific binding was determined with FITC-streptavidin alone. To assess microglia activation, microglia cells (1×10^5 cells per well) were pre-incubated with or without recombinant Gal1 (1-10 μg/ml) for 2 h followed by stimulation with LPS (25-100 ng/ml; Sigma), IFN-γ (10-100 ng/ml; R&D) or IL-4 (10 ng/ml; BD Biosciences) for 24-48 h. Non-specific binding was blocked by incubation with anti-mouse CD16/CD32 antibody (BD Biosciences) for 5 min and then surface stained with various surface markers according to the manufacturer's instructions (BD Biosciences). Cell surface expression of CD45 and CD80 was assessed with Alexa Fluor 647-labeled anti-CD45R (BD Bioscience) and anti-CD80 (e-Biosciences) antibodies. Cells were then analyzed on a LSRII or FACSAria flow cytometer (BD Biosciences).

Co-cultures of Microglia and Neuronal Cells

Neuronal cultures were prepared from E16-16 cortices. Meninges were stripped from the brain and cortices were minced in Ca^{2+}-free HBSS. Neural tissue was digested using the neural tissue dissociation kit (P) (Miltenyi Biotec). The cell suspension was washed and plated at 5×10^4 cells per well on laminin (Invitrogen)-precoated glass cover slips (10 mm diameter, Electron Microscopy Sciences) and cultured in Neurobasal Medium (Sigma) with 2% B27 supplement (Sigma), penicillin (50 U/ml), streptomycin (50 μg/ml), sodium pyruvate (1 mM) and L-glutamine (2 mM) at 37°C and 5% CO_2. Fresh medium was added every 2 days for a total of 7-10 days. To examine the direct effect of Gal1, neurons were cultured with or without recombinant Gal1 (25 μg/ml) for 48 h. For neuro-glial co-cultures, freshly isolated primary microglia or BV-2 cells were cultured in microglia culture medium, pre-incubated with or without recombinant Gal1 (10 μg/ml) for 15 min and further stimulated with our without LPS (100 ng/ml) for 24 h. Stimulated microglia cells (15×10^3 cells per well) were seeded with neuronal cultures and co-cultured for 48 h.

Stereotactic Transfer of Neonatal Microglia, Neonatal Astrocytes and Clodronate-Containing Liposomes

Recipient mice (6-8 weeks old; 5 per group) were anesthetized with ketamine (200 mg per kg) and xylazine (10 mg per kg). Heads were secured in a sterotaxic head frame (Stoelting Co., Wood Dale, IL). A small hole was drilled into the mouse skull, meninges were locally removed with H_2O_2 and a 10 μl Hamilton syringe with a 29-gauge needle was inserted into

NIH-PA Author Manuscript

NIH-PA Author Manuscript

NIH-PA Author Manuscript

the right lateral ventricle. Pre-treated neonatal microglia or neonatal astrocytes (4-5 × 10^5 cells in 10 μl) or clodronate-containing liposomes (7 mg/ml; 5 μl) were injected at a flow rate of 1 μl per min at the following coordinate: anteroposterior, −0.34 mm; lateral, 1.2 mm; dorsoventral, 2.4 mm. After completion of injection, the needle was left in place for aditional 5 min and then withdrawn at a 0.5 mm per minute. The resulting wound was sutured with surgical nylon and mice were inspected daily for post-operational care.

CD45 Phosphatase Activity

BV-2 microglial cells were pre-incubated with LPS (10 ng/ml) at 37°C for 18 h followed by stimulation with recombinant Gal1 (10 μg/ml) for different time periods and CD45 phosphatase activity was determined essentially as described (van Vliet et al., 2006). Briefly, cells were washed with ice-cold PBS and lysed in Ph lysis buffer (20 mM HEPES, pH 7.2, 2 mM EDTA, 2 mM dithiothreitol, 1% (v/v) Nonidet P-40 and 10% (v/v) glycerol containing protease inhibitors). Cellular debris and nuclear material were removed by centrifugation at 20,000 × g for 15 min at 4°C. Phosphatase activity was determined by incubation of 20 μg of lysed proteins for 4 h at 37°C with 2 mM 4-nitrophenyl ph osphate (Roche) in CD45 Ph assay buffer (100 mM HEPES, pH 7.2, 2 mM EDTA and 2 mM dithiothreitol). The resulting color change was assessed at 410 nm. Specificity was determined by the addition of a specific CD45 phosphatase inhibitor (Calbiochem).

Statistical Analysis

Prism software was used for statistical analysis. For comparison of 2 groups, the unpaired Student's *t*-test was used. Significant differences were assumed at the 5% level and represented as *P* values ($P < 0.05$).

Supplementary Material

Refer to Web version on PubMed Central for supplementary material.

Acknowledgments

We thank F. Poirer for *Lgals1*$^{-/-}$ mice, J. Stupirski and C. Leishman for technical assistance and B. Waksman, B. Zhu and M. Rubinstein for helpful discussions. This study was supported by grants from NMSS (RG4530 to GAR and RG3945 to SJK), NIH (AI071448, AI058680 to SJK), an ERP-project scholarship and PhD scholarship of the German National Academic Foundation (to SCS), the Argentinean Agency for Promotion of Science and Technology (to GAR), the Mizutani Foundation for Glycoscience (to GAR), University of Buenos Aires (to GAR), Argentinean National Council Research (to GAR) and Fundación Sales to GAR. We thank Ferioli and Ostry families for donations.

REFERENCES

Anderson AC, Anderson DE, Bregoli L, Hastings WD, Kassam N, Lei C, Chandwaskar R, Karman J, Su EW, Hirashima M, et al. Promotion of tissue inflammation by the immune receptor Tim-3 expressed on innate immune cells. Science. 2007; 318:1141–1143. [PubMed: 18006747]

Barrionuevo P, Beigier-Bompadre M, Ilarregui JM, Toscano MA, Bianco GA, Isturiz MA, Rabinovich GA. A novel function for galectin-1 at the crossroad of innate and adaptive immunity: galectin-1 regulates monocyte/macrophage physiology through a nonapoptotic ERK-dependent pathway. J. Immunol. 2007; 178:436–445. [PubMed: 17182582]

Bax M, García-Vallejo JJ, Jang-Lee J, North SJ, Gilmartin TJ, Hernández G, Crocker PR, Leffler H, Head SR, Haslam SM, et al. Dendritic cell maturation results in pronounced changes in glycan expression affecting recognition by siglecs and galectins. J. Immunol. 2007; 179:8216–8224. [PubMed: 18056365]

NIH-PA Author Manuscript NIH-PA Author Manuscript NIH-PA Author Manuscript

Bitsch A, Schuchardt J, Bunkowski S, Kuhlmann T, Brück W. Acute axonal injury in multiple sclerosis. Correlation with demyelination and inflammation. Brain. 2000; 123:1174–1183. [PubMed: 10825356]

Butovsky O, Ziv Y, Schwartz A, Landa G, Talpalar AE, Pluchino S, Martino G, Schwartz M. Microglia activated by IL-4 and IFN-γ differentially induce neurogenesis and oligodendrogenesis from adult stem/progenitor cells. Mol. Cell. Neurosci. 2006; 31:149–160. [PubMed: 16297637]

Cedeno-Laurent F, Opperman M, Barthel SR, Kuchroo VK, Dimitroff CJ. Galectin-1 triggers an immunoregulatory signature in th cells functionally defined by IL-10 expression. J. Immunol. 2012; 188:3127–3137. [PubMed: 22345665]

Correa SG, Sotomayor CE, Aoki MP, Maldonado CA, Rabinovich GA. Opposite effects of galectin-1 on alternative metabolic pathways of L-arginine in resident, inflammatory, and activated macrophages. Glycobiology. 2003; 13:119–128. [PubMed: 12626408]

Cui YQ, Zhang LJ, Zhang T, Luo DZ, Jia YJ, Guo ZX, Zhang QB, Wang X, Wang XM. Inhibitory effect of fucoidan on nitric oxide production in lipopolysaccharide-activated primary microglia. Clin. Exp. Pharmacol. Physiol. 2010; 37:422–428. [PubMed: 19843098]

Earl LA, Bi S, Baum LG. N- and O-glycans modulate galectin-1 binding, CD45 signaling, and T cell death. J. Biol. Chem. 2010; 285:2232–2244. [PubMed: 19920154]

Garín MI, Chu CC, Golshayan D, Cernuda-Morollón E, Wait R, Lechler RI. Galectin-1: a key effector of regulation mediated by CD4+CD25+ T cells. Blood. 2007; 109:2058–2065. [PubMed: 17110462]

Hirabayashi J, Hashidate T, Arata Y, Nishi N, Nakamura T, Hirashima M, Urashima T, Oka T, Futai M, Muller WE, et al. Oligosaccharide specificity of galectins: a search by frontal affinity chromatography. Biochim. Biophys. Acta. 2002; 1572:232–254. [PubMed: 12223272]

Ilarregui J, Croci DO, Bianco GA, Toscano MA, Salatino M, Vermeulen ME, Geffner JR, Rabinovich GA. Tolerogenic signals delivered by dendritic cells to T cells through a galectin-1-driven immunoregulatory circuit involving interleukin 27 and interleukin 10. Nat. Immunol. 2009; 10:981–991. [PubMed: 19668220]

Jiang HR, Al Rasebi Z, Mensah-Brown E, Shahin A, Xu D, Goodyear CS, Fukada SY, Liu FT, Liew FY, Lukic ML. Galectin-3 deficiency reduces the severity of experimental autoimmune encephalomyelitis. J. Immunol. 2009; 182:1167–1173. [PubMed: 19124760]

Jeon SB, Yoon HJ, Chang CY, Koh HS, Jeon SH, Park EJ. Galectin-3 exerts cytokine-like regulatory actions through the JAK-STAT pathway. J. Immunol. 2010; 185:7037–7046. [PubMed: 20980634]

Kang Z, Altuntas CZ, Gulen MF, Liu C, Giltiay N, Qin H, Liu L, Qian W, Ransohoff RM, Bergmann C, et al. Astrocyte-restricted ablation of interleukin-17-induced Act1-mediated signaling ameliorates autoimmune encephalomyelitis. Immunity. 2010; 32:414–425. [PubMed: 20303295]

Kawanokuchi J, Shimizu K, Nitta A, Yamada K, Mizuno T, Takeuchi H, Suzumura A. Production and functions of IL-17 in microglia. J. Neuroimmunol. 2008; 194:54–61. [PubMed: 18164424]

Kigerl K, Gensel JC, Ankeny DP, Alexander JK, Donnelly DJ, Popovich PG. Identification of two distinct macrophage subsets with divergent effects causing either neurotoxicity or regeneration in the injured mouse spinal cord. J. Neurosci. 2009; 29:13435–13444. [PubMed: 19864556]

Lau KS, Partridge EA, Grigorian A, Silvescu CI, Reinhold VN, Demetriou M, Dennis JW. Complex N-glycan number and degree of branching cooperate to regulate cell proliferation and differentiation. Cell. 2007; 129:123–134. [PubMed: 17418791]

Lehnardt S, Massillon L, Follett P, Jensen FE, Ratan R, Rosenberg PA, Volpe JJ, Vartanian T. Activation of innate immunity in the CNS triggers neurodegeneration through a Toll-like receptor 4-dependent pathway. Proc. Natl. Acad. Sci. USA. 2003; 100:8514–8519. [PubMed: 12824464]

Mirzoeva S, Koppal T, Petrova TV, Lukas TJ, Watterson DM, Van Eldik LJ. Screening in a cell-based assay for inhibitors of microglial nitric oxide production reveals calmodulin-regulated protein kinases as potential drug discovery targets. Brain Res. 1999; 844:126–134. [PubMed: 10536268]

Norling LV, Sampaio AL, Cooper D, Perretti M. Inhibitory control of endothelial galectin-1 on in vitro and in vivo lymphocyte trafficking. FASEB J. 2008; 22:682–690. [PubMed: 17965266]

Offner H, Celnik B, Bringman TS, Casentini-Borocz D, Nedwin GE, Vandenbark AA. Recombinant human beta-galactoside binding lectin suppresses clinical and histological signs of experimental autoimmune encephalomyelitis. J. Neuroimmunol. 1990; 28:177–184. [PubMed: 1694534]

NIH-PA Author Manuscript

NIH-PA Author Manuscript

NIH-PA Author Manuscript

Ohtsubo K, Takamatsu S, Minowa MT, Yoshida A, Takeuchi M, Marth JD. Dietary and genetic control of glucose transporter 2 glycosylation promotes insulin secretion in suppressing diabetes. Cell. 2005; 123:1307–1321. [PubMed: 16377570]

Partridge EA, Le Roy C, Di Guglielmo GM, Pawling J, Cheung P, Granovsky M, Nabi IR, Wrana JL, Dennis JW. Regulation of cytokine receptors by Golgi N-glycan processing and endocytosis. Science. 2004; 306:120–124. [PubMed: 15459394]

Pasquini LA, Millet V, Hoyos HC, Giannoni JP, Croci DO, Marder M, Liu FT, Rabinovich GA, Pasquini JM. Galectin-3 drives oligodendrocyte differentiation to control myelin integrity and function. Cell Death Differ. 2011; 18:1746–1756. [PubMed: 21566659]

Plachta N, Annaheim C, Bissière S, Lin S, Rüegg M, Hoving S, Müller D, Poirier F, Bibel M, Barde YA. Identification of a lectin causing the degeneration of neuronal processes using engineered embryonic stem cells. Nat. Neurosci. 2007; 10:712–719. [PubMed: 17486104]

Ponomarev ED, Maresz K, Tan Y, Dittel BN. CNS-derived interleukin-4 is essential for the regulation of autoimmune inflammation and induces a state of alternative activation in microglial cells. J. Neurosci. 2007; 27:10714–10721. [PubMed: 17913905]

Rabinovich GA, Croci DO. Regulatory circuits mediated by lectin-glycan interactions in autoimmunity and cancer. Immunity. 2012; 36:322–335. [PubMed: 22444630]

Rasmussen S, Wang Y, Kivisäkk P, Bronson RT, Meyer M, Imitola J, Khoury SJ. Persistent activation of microglia is associated with neuronal dysfunction of callosal projecting pathways and multiple sclerosis-like lesions in relapsing remitting experimental autoimmune encephalomyelitis. Brain. 2007; 130:2816–2829. [PubMed: 17890734]

Rotshenker S, Reichert F, Gitik M, Haklai R, Elad-Sfadia G, Kloog Y. Galectin-3/MAC-2, Ras and PI3K activate complement receptor-3 and scavenger receptor-AI/II mediated myelin phagocytosis in microglia. Glia. 2008; 56:1607–1613. [PubMed: 18615637]

Salemi J, Obregon DF, Cobb A, Reed S, Sadic E, Jin J, Fernandez F, Tan J, Giunta B. Flipping the switches: CD40 and CD45 modulation of microglial activation states in HIV associated dementia (HAD). Mol. Neurodegener. 2011; 6:3. [PubMed: 21223591]

Sasaki T, Hirabayashi J, Manya H, Kasai K, Endo T. Galectin-1 induces astrocyte differentiation, which leads to production of brain-derived neurotrophic factor. Glycobiology. 2004; 14:357–363. [PubMed: 14693917]

Stancic M, Slijepcevic D, Nomden A, Vos MJ, de Jonge JC, Sikkema AH, Gabius HJ, Hoekstra D, Baron W. Galectin-4, a novel neuronal regulator of myelination. Glia. 2012; 60:919–935. [PubMed: 22431161]

Storck T, Schulte S, Hofmann K, Stoffel W. Structure, expression, and functional analysis of a Na(+)-dependent glutamate/aspartate transporter from rat brain. Proc. Natl. Acad. Sci. USA. 1992; 89:10955–10959. [PubMed: 1279699]

Stowell SR, Qian Y, Karmakar S, Koyama NS, Dias-Baruffi M, Leffler H, McEver RP, Cummings RD. Differential roles of galectin-1 and galectin-3 in regulating leukocyte viability and cytokine secretion. J. Immunol. 2008; 180:3091–3102. [PubMed: 18292532]

Takeuchi H, Mizuno T, Zhang G, Wang J, Kawanokuchi J, Kuno R, Suzumura A. Neuritic beading induced by activated microglia is an early feature of neuronal dysfunction toward neuronal death by inhibition of mitochondrial respiration and axonal transport. J. Biol. Chem. 2005; 280:10444–10454. [PubMed: 15640150]

Toscano MA, Bianco GA, Ilarregui JM, Croci DO, Correale J, Hernandez JD, Zwirner NW, Poirier F, Riley EM, Baum LG, Rabinovich GA. Differential glycosylation of TH1, TH2 and TH-17 effector cells selectively regulates susceptibility to cell death. Nat. Immunol. 2007; 8:825–834. [PubMed: 17589510]

Toscano MA, Commodaro AG, Ilarregui JM, Bianco GA, Liberman A, Serra HM, Hirabayashi J, Rizzo LV, Rabinovich GA. Galectin-1 suppresses autoimmune retinal disease by promoting concomitant Th2- and T regulatory-mediated anti-inflammatory responses. J. Immunol. 2006; 176:6323–32. [PubMed: 16670344]

Trapp BD, Nave K-A. Multiple sclerosis: an immune or neurodegenerative disorder? Annu. Rev. Neurosci. 2008; 31:247–269. [PubMed: 18558855]

NIH-PA Author Manuscript

NIH-PA Author Manuscript

NIH-PA Author Manuscript

Tsuboi S, Sutoh M, Hatakeyama S, Hiraoka N, Habuchi T, Horikawa Y, Hashimoto Y, Yoneyama T, Mori K, Koie T, et al. A novel strategy for evasion of NK cell immunity by tumours expressing core2 O-glycans. EMBO J. 2011; 30:3173–3185. [PubMed: 21712812]

van der Leij J, van den Berg A, Harms G, Eschbach H, Vos H, Zwiers P, van Weeghel R, Groen H, Poppema S, Visser L. Strongly enhanced IL-10 production using stable galectin-1 homodimers. Mol. Immunol. 2007; 44:506–513. [PubMed: 16581128]

van Vliet SJ, Gringhuis SI, Geijtenbeek TB, van Kooyk Y. Regulation of effector T cells by antigen-presenting cells via interaction of the C-type lectin MGL with CD45. Nat. Immunol. 2006; 7:1200–1208. [PubMed: 16998493]

Venkatesan C, Chrzaszcz M, Choi N, Wainwright MS. Chronic upregulation of activated microglia immunoreactive for galectin-3/Mac-2 and nerve growth factor following diffuse axonal injury. J. Neuroinflamm. 2010; 7:32.

Walther M, Kuklinski S, Pesheva P, Guntinas-Lichius O, Angelov DN, Neiss WF, Asou H, Probstmeier R. Galectin-3 is upregulated in microglial cells in response to ischemic brain lesions, but not to facial nerve axotomy. J. Neurosci. Res. 2000; 61:430–435. [PubMed: 10931529]

Wang Y, Imitola J, Rasmussen S, O'Connor KC, Khoury SJ. Paradoxical dysregulation of the neural stem cell pathway sonic hedgehog-Gli1 in autoimmune encephalomyelitis and multiple sclerosis. Ann. Neurol. 2008; 64:417–427. [PubMed: 18991353]

Weber MS, Prod'homme T, Youssef S, Dun SE, Rundle CD, Lee L, Patarroyo JC, Stuve O, Sobel RA, Steinman L, et al. Type II monocytes modulate T cell-mediated central nervous system autoimmune disease. Nat. Med. 2007; 13:935–943. [PubMed: 17676050]

Wei Q, Eviatar-Ribak T, Miskimins WK, Miskimins R. Galectin-4 is involved in p27-mediated activation of the myelin basic protein promoter. J. Neurochem. 2007; 101:1214–1223. [PubMed: 17403142]

Weiner HL. The challenge of multiple sclerosis: How do we cure a chronic heterogeneous disease? Ann. Neurol. 2009; 65:239–248. [PubMed: 19334069]

Xing B, Xin T, Hunter R, Bing G. Pioglitazone inhibition of lipopolysaccharide-induced nitric oxide synthase is associated with altered activity of p38 MAP kinase and PI3K/Akt. J. Neuroinflamm. 2008; 5:4.

Zamvil SS, Steinman L. Diverse targets for intervention during inflammatory and neurodegenerative phases of multiple sclerosis. Neuron. 2003; 38:685–688. [PubMed: 12797954]

Zhang F, Qian L, Flood PM, Shi JS, Hong JS, Gao HM. Inhibition of IκB kinase-β protects dopamine neurons against lipopolysaccharide-induced neurotoxicity. J. Pharmacol. Exp. Ther. 2010; 3:822–833. [PubMed: 20190013]

NIH-PA Author Manuscript

NIH-PA Author Manuscript

NIH-PA Author Manuscript

HIGHLIGHTS

-Gal1 deactivates classically-activated M1 microglia

-Gal1-glycan interactions promote retention of CD45 on the surface of microglial cells

-Lack of Gal1 favors classical microglia activation, inflammation and neurodegeneration

-Astrocytes control microglia activation and neuroinflammation via Gal1

NIH-PA Author Manuscript
NIH-PA Author Manuscript
NIH-PA Author Manuscript

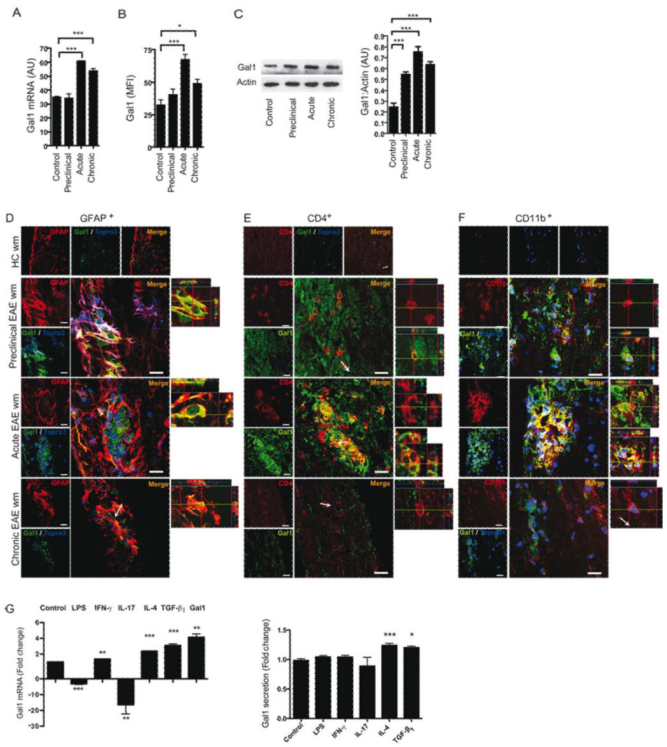

Figure 1. CNS Expression of Gal1 is Dynamically Regulated during EAE

(A-F) Gal1 mRNA and protein expression in mouse spinal cord tissue and confocal microscopy of spinal cord white matter sections from CFA immunized (control), preclinical EAE (preclinical, 10 dpi), acute EAE (acute, 20 dpi) and chronic EAE (chronic, 40 dpi) mice. (A) Relative Gal1 mRNA expression in mouse spinal cord tissue. (B) Mean Fluorescence Intensity (MFI) of Gal1 immunoreactivity in mouse spinal cord white matter. (C) Immunoblot of Gal1 expression in mouse spinal cord tissue. (D-F) Confocal microscopy analysis. Sections were stained with anti-Gal1 antibody (green), the nuclear marker Topro3 (blue) and anti-GFAP (D, red), anti-CD4 (E, red), or anti-CD11b (F, red) antibodies. Scale bars= 20 μm (left panel). Right panels show 3D reconstruction ortho-view micrographs of representative cells. The images of every marker were acquired using the same parameters. (G) Effect of stimulation of astrocytes with LPS (10 ng/ml), IFN-γ (10 ng/ml), IL-17A (10 ng/ml), IL-4 (10 ng/ml), TGF-β_1 (5 ng/ml) and recombinant Gal1 (5 g/ml) on Gal1 mRNA expression and secretion. Data are representative (C-F) or are the mean ± SEM (A,B,C,G) of three independent experiments. *P<0.05; **P<0.01; ***P<0.005 versus control. See also Figure S1.

NIH-PA Author Manuscript
NIH-PA Author Manuscript
NIH-PA Author Manuscript

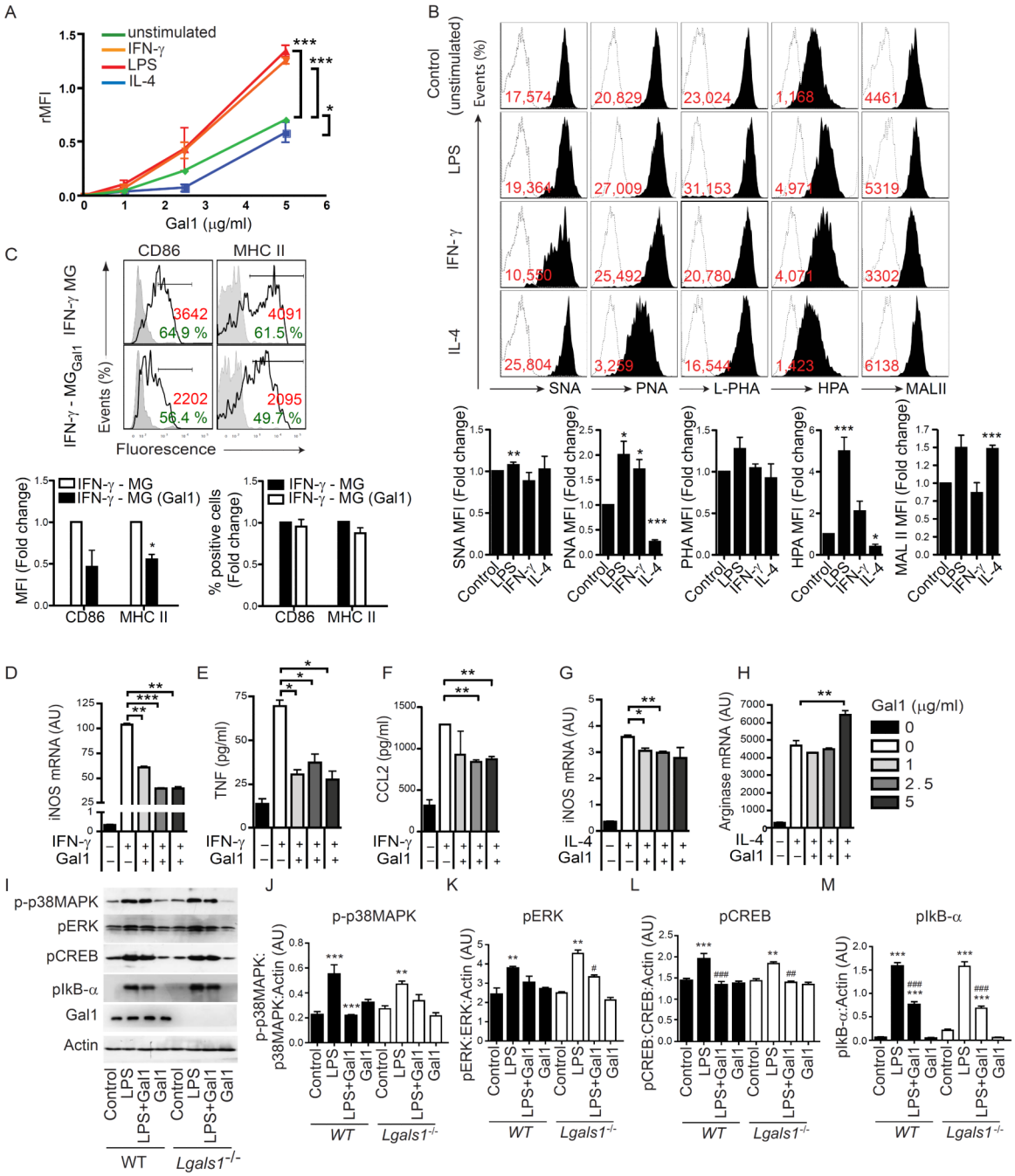

Figure 2. Gal1 Differentially Modulates Microglia Activation *in vitro*

(A) Flow cytometry of resting and polarized microglia subsets incubated with increasing concentrations of recombinant Gal1. (B) Expression of cell surface glycans on M1 (LPS, IFN-γ), M2 (IL-4) and resting (unstimulated) microglia, detected with biotinylated SNA, PNA, L-PHA, HPA and MAL II (black filled histograms) or with FITC-conjugated streptavidin alone (dashed open histograms). Red numbers represent the relative median of intensity (median of intensity (Lectin) – median of intensity (Streptavidin control)). Bar diagrams display the lectin binding as fold change relative to unstimulated microglia. (C) Flow cytometry of M1 microglia activated by IFN-γ (24 h). Control (IFN-γ-MG) or Gal1-treated (IFN-γ-MG_{Gal1}) microglia were stained with antibodies against CD86 and MHC II.

NIH-PA Author Manuscript

NIH-PA Author Manuscript

NIH-PA Author Manuscript

Black lines represent specific antibody binding whereas tinted lines represent unspecific fluorescence signal. Percentage of positive cells and relative median fluorescence (rMFI): (median fluorescence intensity of specific marker signal – median fluorescence intensity of unspecific signal) are shown. Bar diagrams display the relative MFI and percentage of positive cells as fold change relative to IFN-γ-treated microglia. (D-H) Effect of Gal1 on the expression of specific activation markers of IFN-γ- or IL-4-stimulated microglia as determined by quantitative RT-PCR for iNOS (D,G) and arginase (H) mRNA or by bead-based Luminex assay for TNF (E) and CCL2 (F). (I-M) Immunoblot blot (I) and densitometric analysis (J-M) of p-p38MAPK, pERK1/2, pCREB and pIκB-α in neonatal microglia obtained from *Lgals1*$^{-/-}$ or WT mice, pre-treated or not with Gal1 (5 μg/ml) and stimulated with LPS. Data are representative (B and C upper panel, I) or are the mean ± SEM (A-H, J-M) of three independent experiments. **P*<0.05; ***P*<0.01; ****P*<0.005 versus control. See also Figure S2 and S3.

NIH-PA Author Manuscript
NIH-PA Author Manuscript
NIH-PA Author Manuscript

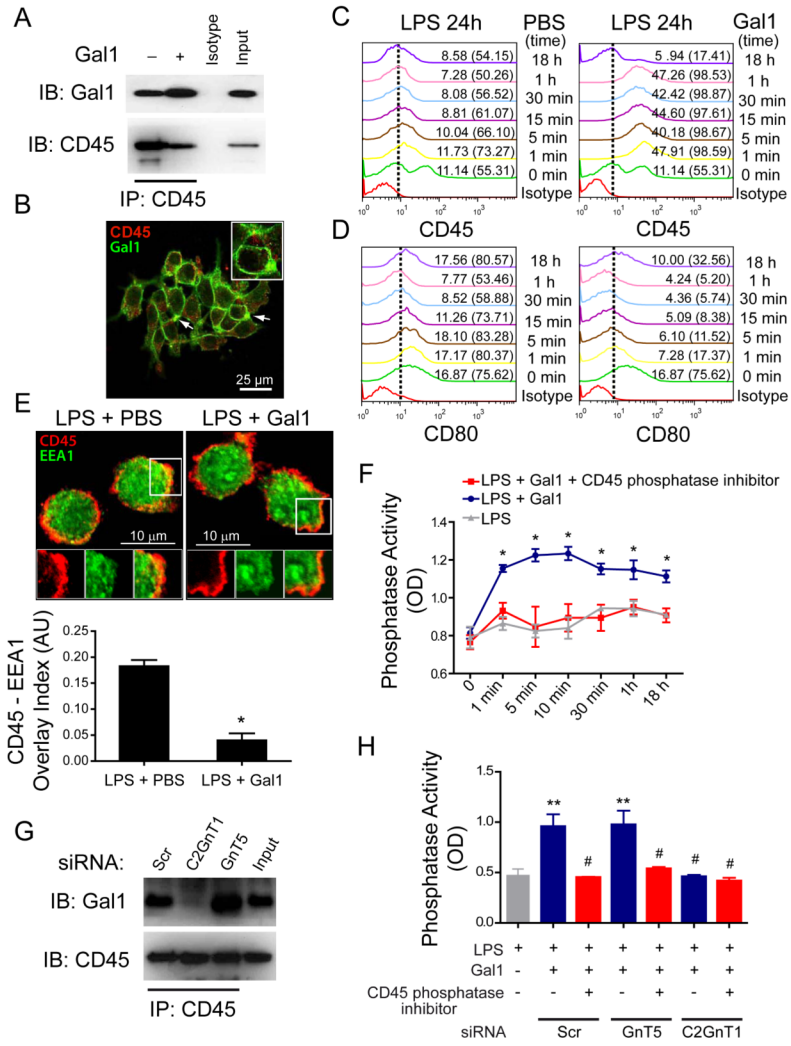

Figure 3. Gal1-glycan Interactions Promote Retention of CD45 on the Surface of Microglial Cells and Augment its Phosphatase Activity

(A) Co-immunoprecipitation followed by immunoblotting of Gal1 and CD45 expression in lysates from microglia cells incubated with LPS (10 ng/ml) for 18 h and further stimulated or not with recombinant Gal1. Input, whole cell lysate; IB, immunoblot; IP, immunoprecipitation. (B) Confocal microscopy of CD45 and Gal1 co-localization in BV-2 microglia cells incubated with LPS for 18 h and further exposed to FITC-conjugated Gal1. Scale bar = 25 m. Inset scale bar = 10 m. (C,D) Flow cytometry analysis of CD45 and CD80 expression in unpermeabilized BV-2 microglia cells incubated with LPS for 18 h and then stimulated with PBS or Gal1 for the indicated time periods. Nonspecific binding determined with isotype-matched control antibodies is shown for treatment at t = 1 min. Numbers outside parentheses show the percentage of positive cells. Numbers in parentheses represent the relative mean fluorescence intensity (rMFI): (median fluorescence intensity of specific marker signal – median fluorescence intensity of unspecific signal) for each time analyzed. (E) Confocal microscopy of CD45 internalization in LPS-stimulated microglia cells treated with Gal1 or vehicle control for 30 min. Cells were fixed, permeabilized and probed with monoclonal antibodies against CD45 and EEA1. Upper panel, representative images of EEA1 (green) - and CD45 (red)-stained microglia cells. Scale bar = 25 m. Inset scale bar = 10 m. Lower panel, CD45/EEA1 overlay normalized to total EEA1 staining determined by

NIH-PA Author Manuscript

NIH-PA Author Manuscript

NIH-PA Author Manuscript

MBF-ImageJ Colocalization Analysis by defining a box of set dimensions and scoring the incidence of superposition in 6 randomly selected areas. (F) CD45-specific phosphatase activity in microglia treated with LPS and further exposed to Gal1 in the absence or presence of a CD45-specific phosphatase inhibitor for the indicated time periods. (G) Co-immunoprecipitation followed by immunoblotting of Gal1 and CD45 expression in lysates from microglia cells transfected with C2GnT1, GnT5 or scrambled (Scr) siRNA, stimulated with LPS (10 ng/ml) and further treated with Gal1. Input, whole cell lysate. Data are representative of two independent experiments. (H) CD45-specific phosphatase activity in microglia cells transfected with GnT5, C2GnT1 or scrambled (Scr) siRNA, treated with LPS and further exposed to Gal1 for 30 min in the absence or presence of a CD45-specific phosphatase inhibitor. Similar results were observed by pre-incubating BV-2 microglia cells with Gal1 before exposure to LPS as in Figure 2. Data are representative (A-E, G) or are the mean ± SEM (E lower panel, F, H) of three independent experiments. $*P<0.05$ versus LPS; $**P<0.01$ versus LPS; $^{\#}P<0.05$ versus LPS plus Gal1. See also Figure S4.

NIH-PA Author Manuscript
NIH-PA Author Manuscript
NIH-PA Author Manuscript

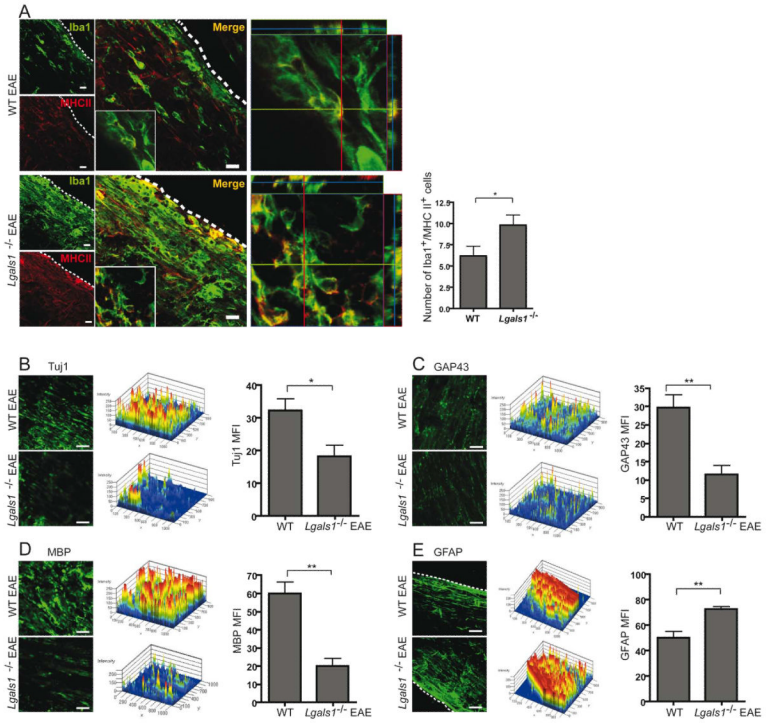

Figure 4. Endogenous Gal1 Controls Classical Microglia Activation *in vivo* and Limits EAE Neuropathology

(A-E) Confocal microscopy of spinal cord white matter of WT and *Lgals1*$^{-/-}$ mice 35 days after immunization with MOG35-55. (A) Left. Spinal cord sections were stained for Iba1 (green) and MHC II (red). Insert shows low magnification micrograph of representative cells. Middle. 3D reconstruction ortho-view of low magnification migrograph. Right. Quantification of MHC II, Iba1 double positive microglia cells (n=20). (B) Left. Spinal cord sections were stained for Tuj1 (green). Middle. 2.5D intensity analysis of Tuj1 staining. Right. mean fluorescence intensity (MFI) of immunoreactivity against Tuj1. (C) Left. Spinal cord sections were stained for GAP43 (green). Middle. 2.5D intensity analysis of GAP43 staining. Right mean fluorescence intensity (MFI) of immunoreactivity against GAP43. (D) Left. Spinal cord sections were stained for MBP (green). Middle. 2.5D intensity analysis of MBP staining. Right mean fluorescence intensity (MFI) of immunoreactivity against MBP. (E) Left. Spinal cord sections were stained for GFAP (green). Middle. 2.5D intensity analysis of GFAP staining. Right mean fluorescence intensity (MFI) of immunoreactivity against GFAP. Scale bars= 20 μm. (A-E) Data are representative (images) or are the mean (bars) ± SEM of three independent experiments. *$P < 0.05$; **$P < 0.01$.

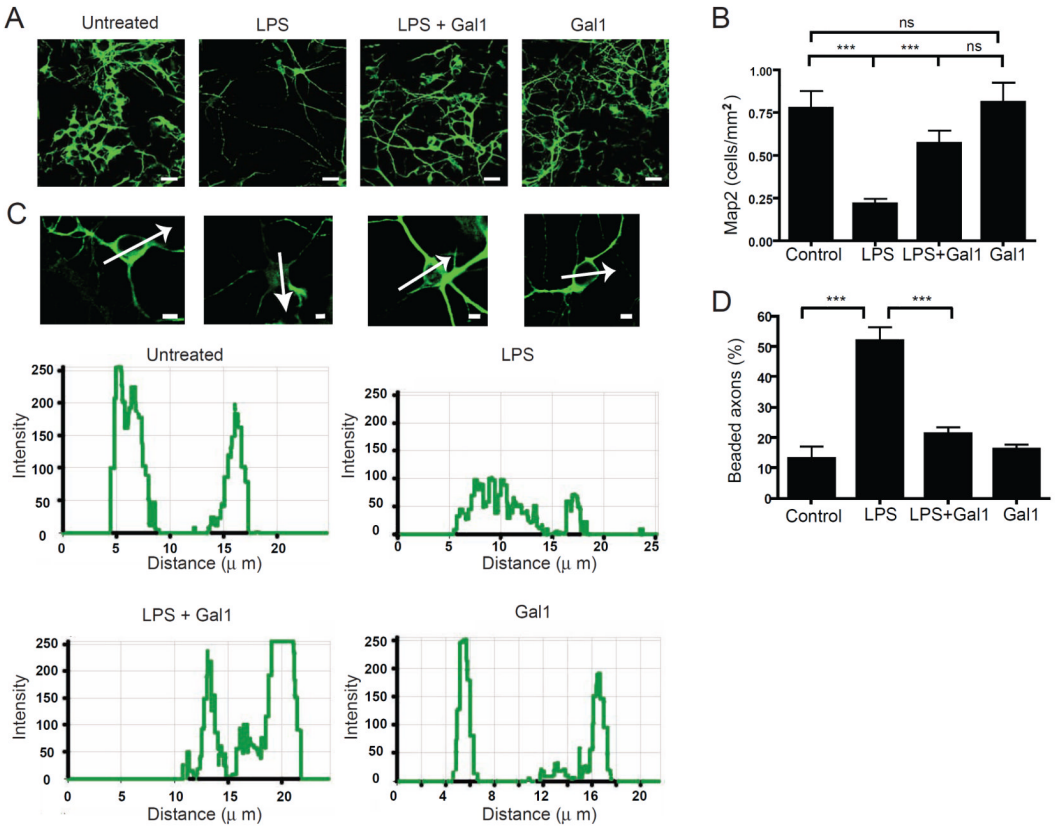

Figure 5. Gal1 Negatively Regulates Microglia-induced Neurotoxicity

(A-D) Twenty four-h co-culture of pre-treated microglia (untreated MG, LPS-treated MG, LPS plus Gal1-treated MG and Gal1-treated MG) with high-density cortical neuronal cultures. (A) Representative fluorescence photomicrographs of $Map2^+$ (green) neurons. (B) Density of $Map2^+$ cell bodies per mm^2 (n=10). (C) High magnification photomicrographs of single $Map2^+$ neurons and pixel intensity analysis (below). (D) Percentage of beaded axons per total axons (n=10) (A) Scale bar= 50 μm, (C) Scale bar= 5 μm. Data are representative (A,C) or are the mean ± SEM (B,D) of three independent experiments. ***$P < 0.005$. See also Figure S5.

NIH-PA Author Manuscript
NIH-PA Author Manuscript
NIH-PA Author Manuscript

NIH-PA Author Manuscript

NIH-PA Author Manuscript

NIH-PA Author Manuscript

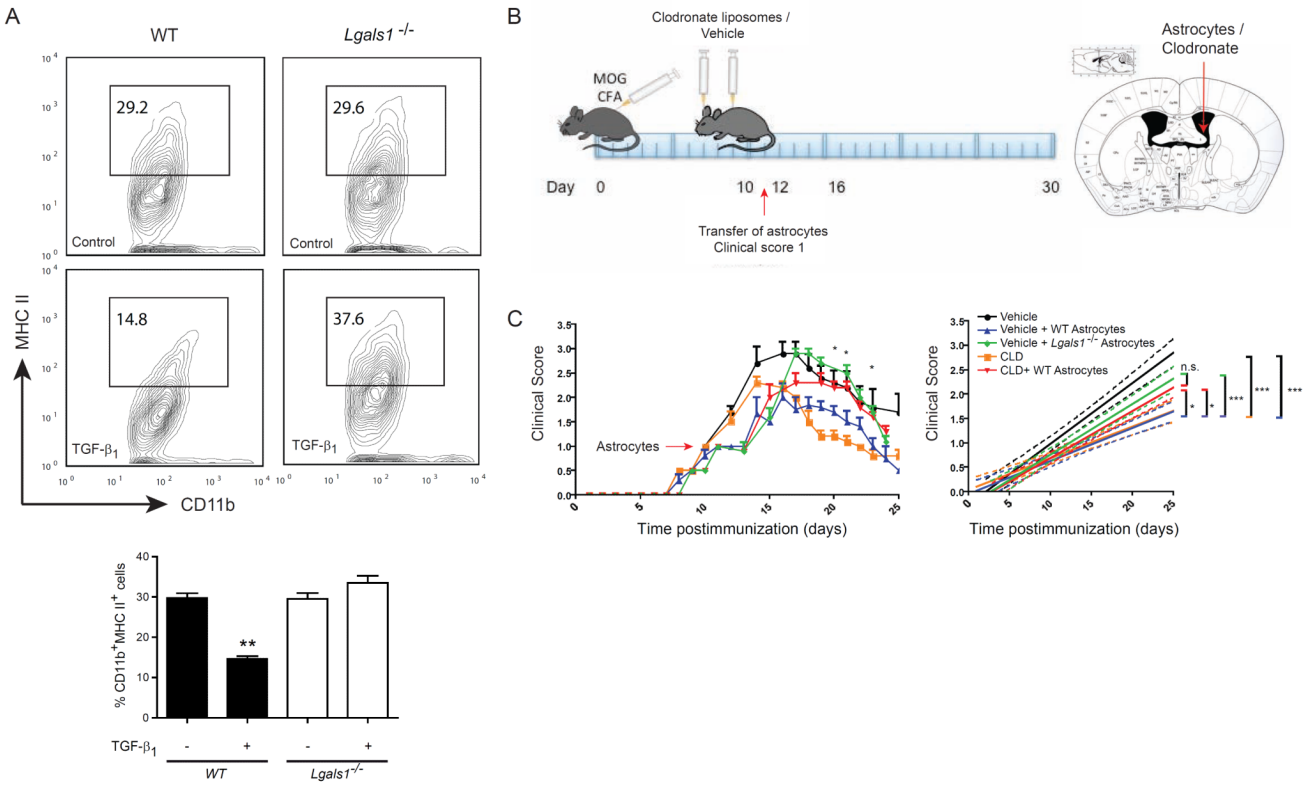

Figure 6. Astrocytes Control Microglia Activation and Limit EAE Severity via Gal1

(A) Flow cytometry of MHC II in cultured CD11b$^+$ microglia. Microglia were exposed to conditioned media from control or TGF-β_1-stimulated WT or *Lgals1*$^{-/-}$ astrocytes. Percentage of CD11b$^+$MHC II$^+$ cells. (B,C) *Lgals1*$^{-/-}$ mice were immunized with 200 μg MOG35-55 and injected with PBS (vehicle) or clodronate-containing liposomes (CLD) into the right lateral ventricle (day 7 and 9 post immunization). When reaching a clinical score of 1, mice were divided into 2 groups and received either WT or *Lgals1*$^{-/-}$ (KO) astrocytes into the same injection site. (B) Diagram illustrating the experimental time line (left) and injection site (right). (C) Clinical score (left) and linear regression curves of disease (right) for each group (dashed lines, 95% confidence intervals). Data are representative (A, upper panel) or are the mean ± SEM (A lower panel, C) of three independent experiments. *$P <$ 0.05; **$P <$ 0.01; ***$P <$ 0.005. See also Figure S6.

NIH-PA Author Manuscript
NIH-PA Author Manuscript
NIH-PA Author Manuscript

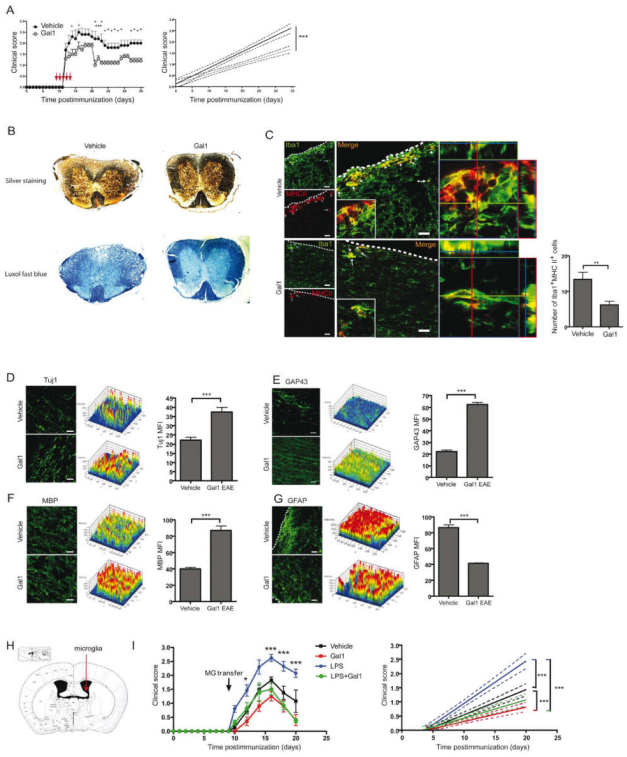

Figure 7. Gal1 Therapy Ameliorates EAE, Limits Microglia Activation, Controls Axonal Loss and Promotes Synaptic Repair

(A) Disease score (left) of vehicle-treated and Gal1-treated (100 μg/ day) mice, immunized with 200 μg MOG35-55 and linear regression curves of disease for each group (right, dashed lines, 95% confidence intervals). (B) Bielschowsky silver (upper panel) and Luxol fast blue (lower panel) staining of spinal cord after 35 days of EAE in Gal1- or vehicle-treated mice. (C-G) Confocal microscopy of spinal cord white matter on day 35 post-immunization in Gal1- or vehicle-treated mice. (C) Left, sections were stained for Iba1 (green) and MHC II (red). Insert shows low magnification micrograph of representative cells. Middle. 3D reconstruction ortho-view of low magnification micrograph. Right, graph represents a quantification of Iba1, MHCII double positive cells in different groups. (D) Left, spinal cord sections were stained for Tuj1 (green). Middle, 2.5D intensity analysis of Tuj1 staining Right, mean fluorescence intensity (MFI) of immunoreactivity against Tuj1. (E) Left, spinal cord sections were stained for GAP43 (green). Middle, 2.5D intensity analysis of GAP43 staining Right, mean fluorescence intensity (MFI) of immunoreactivity against GAP43. (F) Left, spinal cord sections were stained for MBP (green). Middle. 2.5D intensity analysis of MBP staining. Right, mean fluorescence intensity (MFI) of immunoreactivity against MBP. (G) Left, Spinal cord sections were stained for GFAP (green). Middle, 2.5D intensity analysis of GFAP staining. Right, mean fluorescence intensity (MFI) of immunoreactivity against GFAP. (H,I) Neonatal microglia were pre-treated *in vitro* with vehicle, LPS, Gal1 or LPS plus Gal1 for 24 h before transfer to the right lateral ventricle of *Lgals1*$^{-/-}$ EAE mice (day 9 post-immunization; n=6 per group). (H) Diagram illustrating the injection site. (I) Clinical score (left) and linear regression curves of disease for each group (right; dashed lines; 95% confidence intervals). Scale bars = 20 μm. Data are the mean ± SEM (A, C-G, I) or are representative (B-G, images) of four independent experiments. **P*<0.05; ***P*<0.01; ****P*<0.005 versus vehicle. See also Figure S7.